Nonmammalian orthologs of prestin (SLC26A5) are electrogenic divalent/chloride anion exchangers

Thorsten J. Schaechinger and Dominik Oliver*

Institute of Physiology II, University of Freiburg, Hermann-Herder-Strasse 7, 79104 Freiburg, Germany

Edited by Michael J. Welsh, University of Iowa College of Medicine, Iowa City, IA, and approved March 16, 2007 (received for review September 28, 2006)

Individual members of the mammalian SLC26 anion transporter family serve two fundamentally distinct functions. Whereas most members transport different anion substrates across a variety of epithelia, prestin (SLC26A5) is special, functioning as a membrane-localized motor protein that generates electrically induced motions (electromotility) in auditory sensory hair cells of the mammalian inner ear. The transport mechanism of SLC26 proteins is not well understood, and a mechanistic relation between anion transport and electromotility has been suggested but not firmly established so far. To address these questions, we have cloned prestin orthologs from chicken and zebrafish, nonmammalian vertebrates that presumably lack electromotility in their auditory systems. Using patch-clamp recordings, we show that these prestin orthologs, but not mammalian prestin, generate robust transport currents in the presence of the divalent anions sulfate or oxalate. Transport is blocked by salicylate, an inhibitor of electromotility generated by mammalian prestin. The dependence of transport equilibrium potentials on sulfate and chloride concentration gradients shows that the prestin orthologs are electrogenic antiporters, exchanging sulfate or oxalate for chloride in a strictly coupled manner with a 1:1 stoichiometry. These data identify transport mode and stoichiometry of electrogenic divalent/monovalent anion exchange and establish a reliable and simple method for the quantitative determination of the various transport modes that have been proposed for other SLC26 transport proteins. Moreover, the sequence conservation between mammalian and nonmammalian prestin together with a common pharmacology of electromotility and divalent antiport suggest that the molecular mechanism behind electromotility is closely related to an anion transport cycle.

anion transporter | cochlea | electromotility

The SLC26 transporters constitute a relatively novel group of vertebrate anion transporters, which belongs to the large sulfate permease family containing members throughout bacteria, fungi, plants, and animals (1, 2). Although most of the known 10 mammalian members have been identified only recently, pivotal physiological roles have emerged. These roles are illustrated most strikingly by human genetic disorders associated with mutations of SLC26 members. Mutations in SLC26A2 (DTDST) underlie various forms of chondrodysplasias that result from reduced cellular sulfate uptake (3, 4). Mutations in the SLC26A3 gene cause congenital chloride diarrhea, a disease characterized by defective intestinal Cl^-:HCO_3^- exchange (5). Pendred's syndrome, characterized by deafness and thyroid goiter, is caused by defects in SLC26A4 (pendrin) and involves impaired iodide transport in the thyroid (6) and defective ion transport in the inner ear (7). Other functions characterized so far include transport of Cl^-, HCO_3^-, formate, and oxalate in the kidney and in the intestine by SLC26A6 (8–10), and HCO_3^- secretion in the kidney by SLC26A4 (11).

Despite obvious relevance, the mechanisms underlying transport have not been worked out for most SLC26 members so far. Although some seem to specifically mediate transport of divalent anions (SLC26A1, ref. 12; SLC26A2, ref. 13) or show selectivity for monovalents (SLC26A4, refs. 14 and 15), others, like SLC26A3 and SLC26A6, seem to operate in different transport modes depending on substrate availability. Thus SLC26A6 can mediate either electrogenic $1Cl^-$:$2HCO_3^-$ exchange (16) or SO_4^{2-}:Cl^- exchange of unknown stoichiometry (12, 17, 18).

Among all members of this versatile group of transporters, SLC26A5 (prestin) (19) is special, because it has no known transport activity; instead it has been identified as the membrane-based motor protein that generates the rapid contraction-elongation cycles of auditory outer hair cells of the mammalian cochlea, termed electromotility (20, 21). Electromotility is one of possibly two mechanisms contributing to the "cochlear amplifier," an active mechanical process that is crucial for the sensitivity and frequency selectivity of the mammalian ear (22).

The molecular basis of electromotility can be conclusively explained by voltage-dependent conformational rearrangements of prestin, with different conformations occupying different areas in the membrane (23, 24). Aggregate area changes of the large population of prestin molecules densely packed in the lateral membrane of the outer hair cell can alter the overall cell length. Voltage sensitivity of the transition between conformational states requires the movement of an electrically charged particle through the membrane electrical field. In fact, the resultant movement of electrical charge can be measured (20). We have previously shown that this charge movement, as well as electromotility *per se*, requires intracellular monovalent anions, such as Cl^- or HCO_3^-, whereas divalents, such as SO_4^{2-}, alone cannot maintain prestin's activity (25). This finding led us to conclude that voltage sensitivity of prestin may be brought about by the partial translocation of Cl^- or HCO_3^-, which in turn may trigger the major conformational change that generates electromotility. Although such a mechanism fits well with prestin's SLC26 background, other observations are not fully consistent with this simple model (26, 27).

Because electromotility is not observed in nonmammalian vertebrates, we reasoned that functional analysis of nonmammalian prestin orthologs may be revealing in terms of common mechanisms of transport and electromotility. Here, we show that the prestin orthologs from fish and birds mediate coupled divalent:Cl^- exchange. Moreover, the sequence homology to mammalian prestin, the similar sensitivity to salicylate of divalent transport and electromotility, and the anion dependence of electromotility suggest that the mechanism by which prestin generates electromotility in outer hair cells is evolutionary derived from and mechanistically related to divalent:Cl^- antiport.

Author contributions: D.O. designed research; T.J.S. and D.O. performed research; T.J.S. and D.O. analyzed data; and D.O. wrote the paper.

The authors declare no conflict of interest.

This article is a PNAS Direct Submission.

Abbreviations: cPres, chicken prestin; zPres, zebrafish prestin; rPres, rat prestin; V_{rev}, reversal potential; NLC, nonlinear capacitance.

Data deposition: The sequence reported in this paper has been deposited in the GenBank database (accession no. EF028087).

*To whom correspondence should be addressed. E-mail: dominik.oliver@physiologie.uni-freiburg.de.

This article contains supporting information online at www.pnas.org/cgi/content/full/0608583104/DC1.

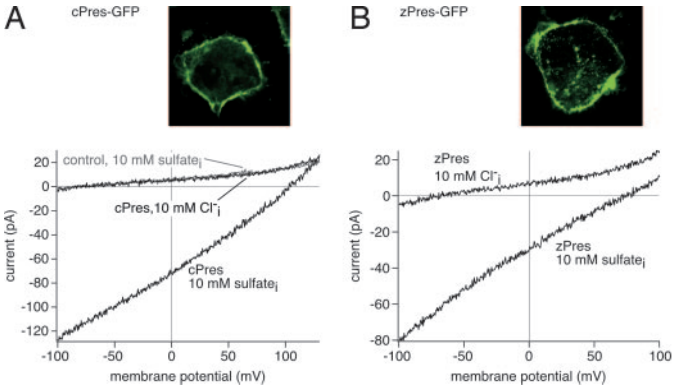

Fig. 1. cPres and zPres expressed in culture cells mediate transport currents in the presence of intracellular sulfate. (*A*) (*Upper*) Transfection of the cPres-GFP construct into cells yields strong plasma membrane fluorescence (opossum kidney cells). (*Lower*) Currents were recorded from CHO cells in response to voltage ramps from −100 to +130 mV. Robust transport currents were measured from cells showing strong plasma membrane cPres-GFP fluorescence with 10 mM SO_4^{2-} (plus 10 mM Cl^-) in the patch pipette. Note the positive V_{rev} (103.4 mV) of the current. In contrast, only endogenous background currents comparable to nontransfected cells were found in the absence of SO_4^{2-}. Nontransfected cells from the same coverslip that completely lacked fluorescence (control, gray trace) did not produce detectable transport currents with $SO_4^{2-}{}_i$. Extracellular solution contained no sulfate. (*B*) (*Upper*) Strong plasma membrane localization of expressed zPres-GFP (opossum kidney cells). (*Lower*) Transport currents measured from CHO cells with similar levels of zPres-GFP membrane fluorescence in the presence of 10 mM $SO_4^{2-}{}_i$ (+10 mM $Cl^-{}_i$), but not with 10 mM $Cl^-{}_i$ alone.

Results

The chicken ortholog to mammalian prestin (cPres) was cloned from chicken inner ear by using RACE-PCR. cPres shows substantial overall homology to rat prestin (rPres) (58% amino acid identity) and the previously described ortholog from zebrafish (zPres) (refs. 28 and 29; 59% identity). Hydrophobicity analysis indicates a common topology for the SLC26a5 isoforms from all three taxa [supporting information (SI) Fig. 6]. Sequence conservation is highest in the central hydrophobic region presumably harboring 10–12 transmembrane segments (68% identity between cPres and rPres). Both cPres and zPres were robustly targeted to the plasma membrane when expressed in CHO or opossum kidney cells (Fig. 1).

Because some members of the SLC26 family may be electrogenic anion transporters (12, 16–18), we examined cells expressing cPres-GFP for transport currents under voltage clamp in the whole-cell patch-clamp configuration. Cells with strong, unambiguous membrane fluorescence were selected for electrophysiological recordings. When intracellular and extracellular solutions contained only monovalent anions, CHO cells with strong membrane expression of cPres did not exhibit any detectable current ($n = 17$) above the small background conductance found in control cells lacking cPres ($n = 10$). This lack of current also persisted in the presence of a Cl^- concentration gradient across the membrane ($n = 12$; Fig. 1*A*), indicating the absence of electrogenic Cl^- transport. In contrast, robust ionic currents were recorded from all cPres-expressing cells, when the intracellular solution included the divalent anion SO_4^{2-} (10 mM; $n = 25$). These currents had amplitudes of up to 250 pA at −100 mV and were characterized by low noise levels, a nearly linear current-voltage relation, and a positive reversal potential (V_{rev}; Fig. 1*A*). Whereas such currents were never found in control cells lacking cPres ($n = 14$; Fig. 1*A*), similar SO_4^{2-}-dependent currents were also recorded in CHO cells expressing the zebrafish ortholog ($n = 6$; Fig. 1*B*). These results are fully consistent with electrogenic SO_4^{2-} transport by cPres and zPres.

We thus attempted to clarify the exact transport mode underlying these currents. Transport mode and stoichiometry of electrogenic transport can be derived from the V_{rev} of transport currents independent of the detailed transport mechanism (e.g., refs. 30 and 31). V_{rev} is the voltage at which the transport reaction is at thermodynamic equilibrium (equilibrium potential) and hence current is zero. By changing extracellular anion concentrations, we found V_{rev} to depend on both $[Cl^-]$ and $[SO_4^{2-}]$.

In cells expressing cPres, increasing the extracellular $[Cl^-]$ in the presence of a constant SO_4^{2-} concentration gradient shifted V_{rev} to positive potentials (Fig. 2 *A* and *B*). This Cl^- dependence suggests that either Cl^- acts as a regulator of SO_4^{2-} transport or that Cl^- is transported by cPres. The former hypothesis can be ruled out, because the transport equilibrium of selective SO_4^{2-} transport cannot depend on Cl^- (Fig. 2*B*, gray line). Instead, Cl^- must be transported in the presence of SO_4^{2-} to influence V_{rev}. As an alternative hypothesis, one may thus consider a pure Cl^- transport that is activated by the presence of SO_4^{2-}. However, the $[Cl^-]$ dependence of a simple Cl^- permeability is given by the Nernst equation and must yield more negative V_{rev} with increasing $[Cl^-]_{ex}$ (Fig. 2*B*, dashed line; slope −58 mV), exactly contrary to the observed +56.7 mV per 10-fold increase in $[Cl^-]_{ex}$ ("anti-Nernstian" behavior). Similarly, coupled or uncoupled cotransport of both Cl^- and SO_4^{2-} must yield more negative V_{rev} with increasing $[Cl^-]_{ex}$. In contrast to the transport modes considered above, the data completely match predictions (see *SI Text*) for stoichiometric exchange of one sulfate ion for one Cl^- ion (Fig. 2*B*, solid line). For coupled antiport, V_{rev} is given by:

$$V_{rev} = \frac{1}{1 - 2r}\,(E_{Cl} - 2rE_{SO4}),$$

where E_{Cl} and E_{SO4} are the Nernst equilibrium potentials for both anions, and r is the coupling ratio n/m, where m and n denote the stoichiometric numbers of Cl^- and sulfate ions, respectively, transported per exchange cycle (see *SI Text*). In fact, the data are compatible only with a $1SO_4^{2-}{:}1Cl^-$ transport stoichiometry (Fig. 2*C*), whereas other transport ratios either produce different slopes of $V_{rev}([Cl^-]_{ex})$ or are not electrogenic at all ($1SO_4^{2-}{:}2Cl^-$). The anti-Nernstian behavior of the transport currents can be rationalized most easily when considering that for every Cl^- transported in one direction, one net negative charge is going the opposite way, thus reversing the concentration dependence of V_{rev}.

To verify this model, we next changed extracellular $[SO_4^{2-}]$ in the presence of a constant $[Cl^-]$ gradient. As shown in Fig. 2 *D* and *E*, V_{rev} hyperpolarized with increasing $[SO_4^{2-}]_{ex}$. The slope of −56.3 mV per 10-fold change in $[SO_4^{2-}]_{ex}$ quantitatively matched stoichiometric antiport but not pure SO_4^{2-} or Cl^- transport.

Similar results were obtained with zPres. When the Cl^- concentration gradient was altered by changing $[Cl^-]_{ex}$, V_{rev} changed according to $1SO_4^{2-}{:}1Cl^-$ antiport (+51.6 mV per 10-fold increase of $[Cl^-]_{ex}$), but was incompatible with other transport modes (Fig. 2*F*).

These findings unambiguously characterize the nonmammalian prestin isoforms as stoichiometric $1SO_4^{2-}{:}1Cl^-$ exchangers.

Having established transport mode and stoichiometry, we next examined the substrate specificity for divalents. As shown for cPres in Fig. 3, inclusion of the dicarboxylate, oxalate, in the intracellular solution induced transport currents with a positive V_{rev}, similar to SO_4^{2-} transport. Currents measured with intracellular oxalate were larger than sulfate transport currents measured from the same cell, indicating higher transport rates for oxalate. In contrast, the larger dicarboxylate, malonate, did not induce any current (Fig. 3), indicating selectivity of cPres for

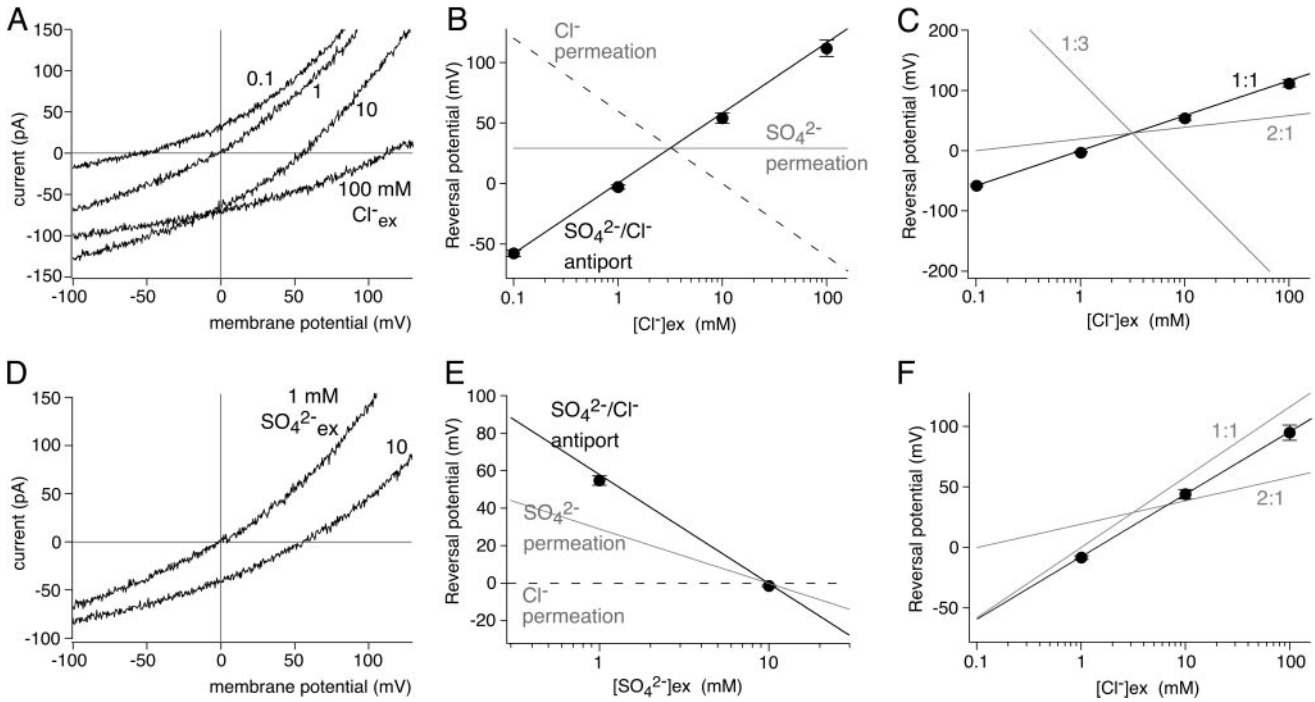

Fig. 2. cPres mediates SO_4^{2-}:Cl^- antiport with a 1:1 stoichiometry. (*A*) Current recordings from CHO cells expressing cPres-GFP with intracellular 10 mM SO_4^{2-} + 10 mM Cl^- and extracellular 1 mM SO_4^{2-} at the various $[Cl^-]_{ex}$ indicated. Note the changed V_{rev} with changed $[Cl^-]_{ex}$. Leak currents were removed by subtraction of currents remaining after application of 10 mM salicylate for each $[Cl^-]_{ex}$. Traces with 1, 10, and 100 mM Cl^- are subsequent recordings from the same cell. (*B*) Mean V_{rev} of leak-subtracted transport currents (n = 4, 14, 10, and 13 cells for 0.1, 1, 10, and 100 mM Cl^-, respectively). Note that the data points closely match the predicted equilibrium potentials of coupled SO_4^{2-}:Cl^- exchange (continuous line; for model, see *SI Text*). In contrast, Cl^- transport (dashed line: Nernst equation) predicts the opposite behavior, whereas equilibrium potentials of pure sulfate transport do not depend on $[Cl^-]$ (gray line). (*C*) The data points from *B* closely match the predicted equilibrium potentials of 1:1 SO_4^{2-}:Cl^- exchange (black line, replotted from *B*), but not of other stoichiometries like 1:3 or 2:1. (*D*) Leak-subtracted transport currents from a cPres-expressing CHO cell, measured as in *A* but with a fixed Cl^- gradient while setting extracellular $[SO_4^{2-}]$ to either 1 or 10 mM. Intracellular and extracellular $[Cl^-]$ and intracellular $[SO_4^{2-}]$ were kept at 10 mM. (*E*) Mean V_{rev} from n = 4 cells measured as in *D*. A linear regression through the average data (not shown) yields a slope of −56.3 mV per 10-fold change in $[SO_4^{2-}]_{ex}$, matching the prediction for coupled 1SO_4^{2-}:1Cl^- exchange (black line; see *SI Text*), but not the Nernstian behavior of simple sulfate transport (gray line), whereas pure Cl^- transport would not be affected by changing $[SO_4^{2-}]_{ex}$ at all (dashed line). (*F*) Mean V_{rev} of transport currents from CHO cells expressing zPres at various $[Cl^-]_{ex}$ (n = 6). Solutions were as in *A*. Currents were recorded and analyzed as in *A* and *B*. A linear fit (solid line) yielded a slope of 51.6 mV per 10-fold increase in $[Cl^-]_{ex}$, matching coupled 1SO_4^{2-}:1Cl^- exchange, but not other exchange stoichiometries.

SO_4^{2-} and oxalate. The same specificity for the divalent substrate was found for zPres.

Specific inhibitors of anion transporters are largely lacking. However, the electromotile function of mammalian prestin is blocked by the amphiphilic anion salicylate at millimolar concentrations (25, 32). We therefore tested for salicylate sensitivity of anion transport by cPres and zPres. Application of salicylate via the extracellular solution blocked transport currents in a dose-dependent and readily reversible manner. The dose-inhibition relation obtained for cPres was characterized by a half-blocking concentration of 1.43 mM and a Hill coefficient of 0.99 (Fig. 4). Strikingly, these values are very similar to the salicylate sensitivity of prestin-mediated electromotility (32).

We finally examined whether mammalian prestin also mediates divalent anion exchange. Currents recorded from CHO cells expressing rPres-GFP in the presence of 10 mM intracellular sulfate or oxalate showed no difference in amplitude or V_{rev} to recordings in the presence of Cl^- alone (Fig. 5). This lack of transport currents was not caused by insufficient membrane expression of rPres, because cells showed robust membrane fluorescence and proper function was verified by measuring the bell-shaped nonlinear capacitance (NLC) generated by prestin (Fig. 5 *Inset*) (25, 32). Moreover, currents from cells expressing rPres were insensitive to salicylate and were not correlated to the amount of NLC, identifying them as background currents not related to transport by prestin. These data indicate, that in contrast to its nonmammalian orthologs, mammalian prestin does not mediate electrogenic transport of sulfate and oxalate.

Discussion

Transport Mechanism. Our results show that two novel members of the SLC26 family mediate 1:1 stoichiometric divalent:Cl^- exchange. Transport mode and stoichiometry were determined quantitatively on a strict biophysical ground by using the thermodynamic equilibrium potentials of electrogenic transport. The main requirements for the precise determination of equilibrium potentials were high expression levels, very tight whole-cell recordings, and the ability to isolate pure transport currents from background leak with a reversible blocker of transport, salicylate.

Because little is known about transport mechanisms underlying SLC26 function, this technically rather simple approach should be helpful for understanding the molecular physiology of the other SLC26 members. So far, most studies on SLC26 have used ion flux assays with radioactively labeled substrates. Such measurements do not readily translate into transport stoichiometries. However, quantitative electrochemical measurements of ion fluxes in *Xenopus* oocytes have recently been used to pin down the stoichiometry for Cl^-:HCO_3^- antiport by SLC26A3 and SLC26A6 (16). In contrast, although transport of SO_4^{2-} (SLC26A1/2; refs. 13 and 33) and oxalate (SLC26A6; refs. 9, 10, 17, and 18) is the physiologically crucial function of some SLC26 proteins, modes and stoichiometry of divalent transport have not

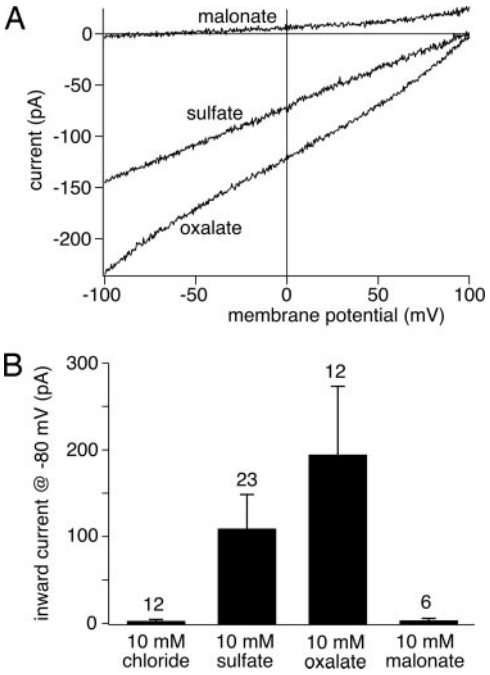

Fig. 3. cPres transports sulfate and oxalate, but not malonate. (*A*) Representative currents recorded from cPres-expressing cells as in Fig. 1 show divalent transport when the patch pipette contained 10 mM SO_4^{2-} or 10 mM oxalate. In contrast, no transport current was recorded with 10 mM intracellular malonate. (*B*) Mean current amplitudes at −80 mV from experiments as in *A*, with pipette solution containing either 10 mM Cl^-, 10 mM SO_4^{2-} + 10 mM Cl^-, 10 mM oxalate + 10 mM Cl^-, or 10 mM malonate + 10 mM Cl^-.

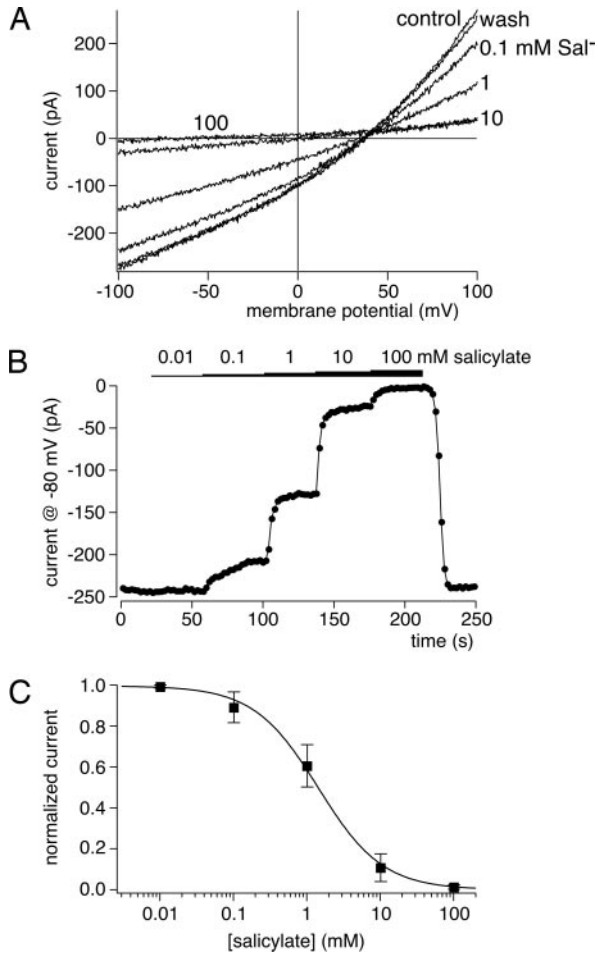

Fig. 4. Salicylate is a reversible blocker of SO_4^{2-}/Cl^- antiport by cPres. (*A*) Transport currents were recorded from a cPres-expressing CHO cell in the presence of the extracellular salicylate concentrations indicated. Salicylate replaced equal concentrations of gluconate in the extracellular solution (intracellular, 10 mM Cl^-, 10 mM SO_4^{2-}; extracellular, 10 mM Cl^-, 1 mM SO_4^{2-}). (*B*) Time course of currents (at −80 mV) from the same experiment as in *A*. Note that inhibition of transport is readily reversible. (*C*) Dose–response relation for salicylate inhibition of cPres-mediated transport currents measured as in *A* and *B* from seven cells. Data from individual cells were normalized to unblocked current amplitude before averaging. Continuous line is a fit of the Hill equation to the mean normalized amplitudes (see *Results*).

been determined yet. So far, it is only clear that oxalate transport by SLC26A6 is electrogenic (12, 17, 18), whereas for the essential mammalian SO_4^{2-} transporters SLC26A1 and SLC26A2 (4, 33), transport mode and electrogenicity are unknown. Their dependence on monovalent anions suggests that they may exchange SO_4^{2-} for HCO_3^- (SLC26A1; refs. 34 and 35) or Cl^- (SLC26A2; ref. 13). Measurement of equilibrium potentials of transport currents should thus provide a straightforward way to reveal whether these transporters operate in the same divalent:monovalent exchange mode identified here for nonmammalian prestin.

Inhibition of transport currents establishes salicylate as a novel inhibitor of SLC26 transporters. Although it remains to be seen whether salicylate also blocks other SLC26 isoforms and transport modes like Cl^-:HCO_3^- exchange, it is known that salicylate inhibits SO_4^{2-}:HCO_3^- exchange in renal and placental epithelia (36, 37). In fact, the half-blocking concentration for tubular basolateral SO_4^{2-} transport is ≈1 mM (36), similar to the value determined in the present study. Basolateral transport in the proximal tubule is most likely mediated by SLC26A1 (38, 39); therefore, it is conceivable that salicylate acts on this transporter in its native environment. Salicylate sensitivity may thus turn out as a general feature of SLC26-mediated anion exchange.

An additional conclusion from our experiments is that transport by prestin does not require consumption of ATP, because all of our intracellular solutions did not contain ATP. Moreover, ATP-dependent processes like ongoing phosphorylation are also not required to keep the transporter in an active state. In fact, transport could be measured for >30 min after establishing whole-cell configuration without rundown of the transport current, a time sufficient to completely deplete the cytoplasm from the readily diffusible ATP (40).

A Role for Anion Transport in Nonmammalian Ears? The zPres ortholog is expressed in inner ear mechanosensory hair cells (28, 29). A similar localization in the chicken is not unlikely because we cloned the cDNA from inner ear tissue. The presence of the prestin transporter in nonmammalian hair cells makes sense in evolutionary terms: a protein already present in the hair cells of phylogenetic ancestors to mammals may have adopted a novel, electromotile function during evolution toward the mammalian outer hair cell. Interestingly, spontaneous otoacoustic emissions from the gecko's ear are salicylate-sensitive (41). In light of our present results, this effect on otoacoustic emissions may result from blocking prestin expressed in the inner ear. As emissions in the nonmammals are believed to result from mechanical amplification provided by hair bundles (41, 42), proper hair cell function may indeed rely on anion transport via the prestin ortholog. However, the localization and function of cPres in the chicken remain to be addressed.

Relation of Prestin-Mediated Electromotility to Anion Antiport. The current results give important clues to the molecular mechanism underlying the electromotile function of mammalian prestin.

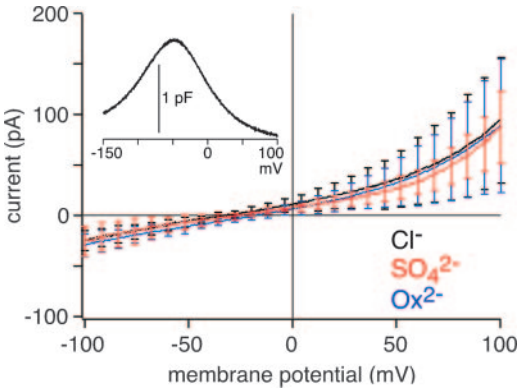

Fig. 5. No electrogenic divalent anion transport by mammalian prestin was found. Average currents recorded from CHO cells expressing rPres with intracellular solutions containing 10 mM Cl^- (black; $n = 8$ cells), 10 mM Cl^- + 10 mM sulfate (red; $n = 8$), or 10 mM Cl^- + 10 mM oxalate (blue; $n = 8$) are shown. Solutions were the same as in Fig. 1. Note that the addition of sulfate or oxalate did not increase currents nor change V_{rev}. (*Inset*) rPres-induced NLC measured from a typical cell with 160 mM $[Cl^-]_i$, before probing transport (average peak NLC = 0.92 ± 0.39 pF).

Several aspects of prestin's function show striking similarities when compared with SO_4^{2-}:Cl^- antiport by cPres/zPres. First, voltage sensitivity and the resultant conformational rearrangements of mammalian prestin depend on the presence of millimolar $[Cl^-]_i$ (25, 27). Binding of the monovalent anion could be to the same binding sites involved in Cl^- transport by nonmammalian prestin. Second, salicylate block of mammalian prestin quantitatively equals the inhibition of nonmammalian transport (32). Third, zPres generates voltage-dependent charge movements (28) resembling the gating charge associated with electromotility. Finally, mammalian and chicken isoforms share a substantial degree of sequence conservation, especially in the hydrophobic core region that presumably provides the structural basis for ion transport. These similarities strongly suggest that prestin's unique function evolved as a modification of an anion exchange mechanism. We propose that electromotility might arise from an incomplete anion transport cycle. Given the obvious dependence on monovalent intracellular anions together with the lack of transport of divalent anions, it seems possible that the specific function of mammalian prestin results from the inability to bind or transport sulfate, resulting in a "defective" transporter that can still bind and possibly partially translocate Cl^- from the intracellular side, but cannot proceed fully to the exposition of the binding site(s) at the extracellular face. Recently, Muallem and Ashmore (43) proposed an electrogenic transport model to account for the voltage and concentration dependence of prestin's charge movement. Most available data were reasonably described by a model that implements the exchange of one Cl^- for one SO_4^{2-} ion, which is exactly the transport mode determined here for nonmammalian prestin. Although we show here that mammalian prestin does not transport sulfate at measurable rates, a truncated version of this type of transport cycle may explain the specific behavior of mammalian prestin.

Materials and Methods

Molecular Biology. Inner ears were dissected from prehatch chicken (embryonic day 20). mRNA was isolated from inner ear tissue with a Dynabeads mRNA DIRECT Kit (Invitrogen, Carlsbad, CA). 5′ and 3′ RACE-Ready cDNAs were then generated with the SMART RACE cDNA Amplification Kit (Clontech, Mountain View, CA). Gene-specific primers for the isolation of prestin were designed according to the predicted coding sequence derived from genomic sequence data (GenBank accession no. XM_415959.1): 5′-AGCTGAAACTCCTGTGCCGATAATGA-3′ for the 5′-RACE; 5′-CTAGCCGATACAGTGGACCCCTCTC-3′ and 5′-CGTCACTGAACGGCTATACCCTGATTGAAGG-3′ to amplify the central and 3′ portion of the cDNA. Both fragments were cloned into pBluescript SK$^-$ (Stratagene, La Jolla, CA) and sequenced. The obtained coding sequence slightly deviated from the predicted one, thus the final cDNA was amplified with the primers 5′-ATGGAAGATGCTCAAGAAAGTGGAGAGTGTC-3′ and 5′-GTGGTCTAAGGCAGTCTGTGAAGCAGACC-3′ and subsequently cloned into the expression vector pEGFP-N1 (Clontech). The cPres sequence was deposited in GenBank (accession no. EF028087).

Confocal Fluorescence Microscopy. Opossum kidney cells were grown in DMEM/F12 containing 10% FCS and 1% penicillin/streptomycin solution. Cells were transfected with Lipofectamine 2000 (Invitrogen), fixed after 24 h with 4% paraformaldehyde in PBS for 10 min at 4°C, washed, and mounted in Aquapolymount (Polysciences, Warrington, PA). Confocal microscopy was done on Laser Scanning Microscope 510 NLO (Zeiss, Jena, Germany).

Electrophysiology. The expression plasmids pEGFP-N1-cPres, pEGFP-N1-zPres (GenBank accession no. NP-958881; ref. 28), or pEGFP-N1-rPres were transfected into CHO cells by using the JetPEI transfection reagent (Polyplus, Illkirch, France). For electrophysiological experiments (24–48 h after transfection), cells with unequivocal membrane fluorescence observed under wide-field fluorescence illumination (488 nm) were selected. Nonexpressing cells from the same coverslip that completely lacked fluorescence were chosen as controls.

Whole-cell patch-clamp recordings were carried out at room temperature (22–24°C) with an EPC10 amplifier (Heka, Lambrecht, Germany) controlled by the Patchmaster software (Heka). Electrodes were pulled from quartz glass and had resistances of 1.5–3.5 MΩ. Whole-cell series resistances ranged from 2 to 10 MΩ.

Electrodes were filled with one of the following solutions: 160 mM CsCl; 10 mM CsCl, 150 mM K-aspartate; 10 mM CsCl, 130 mM K-aspartate, 10 mM Cs_2SO_4; 10 mM CsCl, 130 mM K-aspartate, 10 mM Cs_2-oxalate; or 10 mM CsCl, 130 mM K-aspartate, 10 mM Cs_2-malonate. All intracellular solutions contained 1 mM Hepes and 1 mM K_2 EGTA and were adjusted to pH 7.3 with KOH.

Unless specified otherwise, extracellular solution was 144 mM NaCl, 5.8 mM KCl, 1.3 mM $CaCl_2$, 0.9 mM $MgCl_2$, 10 mM Hepes, 0.7 mM Na_2HPO_4, and 5.6 mM glucose, pH 7.4 (NaOH). For experiments with specific extracellular monovalent and divalent concentrations, the following different extracellular solutions were applied via a glass capillary positioned close to the cell. For changing $[Cl^-]_{ex}$, the basic composition was 160 mM Na-gluconate and 1 mM Cs_2SO_4; the indicated concentrations of Cl^- were added as NaCl at the expense of Na-gluconate. For exchanging $[SO_4^{2-}]_{ex}$, solutions contained either 10 mM CsCl, 149 mM Na-gluconate, 1 mM Cs_2SO_4 or 10 mM CsCl, 140 mM Na-gluconate, and 10 mM Cs_2SO_4. For salicylate dose–response measurements the extracellular solution contained 10 mM CsCl, 149 mM Na-gluconate, and 1 mM Cs_2SO_4, and the specified concentrations of Na-salicylate replaced equal concentrations of Na-gluconate. All extracellular solutions additionally contained 2 mM Ca-gluconate and 5 mM Hepes and were adjusted to pH 7.4 with NaOH. Whenever extracellular solutions were changed, an agar bridge was used as the bath electrode.

Currents were recorded in response to command voltage ramps from −100 mV to +100 mV or +130 mV and plotted against membrane potential. Currents traces shown are averages

of 3 to 10 subsequent individual recordings. For the precise determination of V_{rev}, leak currents had to be subtracted, as the small endogenous currents (e.g., Fig. 1) resulted in a substantial left-shift of V_{rev}. Therefore, for each ionic condition, 10 mM salicylate was applied and pure transport current was determined by subtracting the residual current in the presence of salicylate from the overall current. Note that inhibition of transport by salicylate was rapidly reversible (see Fig. 4*B*; complete washout within 20 s). Salicylate was washed out with the same solution preceding its application, and residual currents were subtracted from unblocked currents recorded immediately before or after salicylate application. In some cells (including control cells) a substantial outwardly rectifying current beyond +50 mV that developed with recording time was eliminated in this manner. Moreover in some cases, especially when transport currents were large and the series resistance was relatively high, V_{rev} showed slow drifts, indicative of changes of substrate concentrations caused by the transport. These artefacts were minimized by largely canceling the steady-state transport occurring between voltage ramps. This canceling was achieved by manually adjusting the holding potential at each ionic condition to approximately match the zero-current potential of transport.

The NLC of cells expressing rPres was measured by using a lock-in technique as described (25, 28).

All data were analyzed with IgorPro and are given as mean ± SD.

We thank M. Knipper (University of Tübingen, Tübingen, Germany) for the zPres clone, M. Scaal (University of Freiburg) for the chicken tissue, E. Reisinger for help with the RACE technology, and B. Fakler and C. Fahlke for helpful discussions. This work was supported by European Union Grant LSHG-CT-2004-512063 (Eurohear).

1. Mount DB, Romero MF (2004) *Pflügers Arch* 447:710–721.
2. Saier MH, Jr, Tran CV, Barabote RD (2006) *Nucleic Acids Res* 34:D181–D186.
3. Dawson PA, Markovich D (2005) *Curr Med Chem* 12:385–396.
4. Hastbacka J, de la Chapelle A, Mahtani MM, Clines G, Reeve-Daly MP, Daly M, Hamilton BA, Kusumi K, Trivedi B, Weaver A, *et al.* (1994) *Cell* **78,** 1073–1087.
5. Hoglund P, Haila S, Socha J, Tomaszewski L, Saarialho-Kere U, Karjalainen-Lindsberg ML, Airola K, Holmberg C, de la Chapelle A, Kere J (1996) *Nat Genet* 14:316–319.
6. Everett LA, Glaser B, Beck JC, Idol JR, Buchs A, Heyman M, Adawi F, Hazani E, Nassir E, Baxevanis AD, *et al.* (1997) *Nat Genet* 17:411–422.
7. Royaux IE, Belyantseva IA, Wu T, Kachar B, Everett LA, Marcus DC, Green ED (2003) *J Assoc Res Otolaryngol* 4:394–404.
8. Tuo B, Riederer B, Wang Z, Colledge WH, Soleimani M, Seidler U (2006) *Gastroenterology* 130:349–358.
9. Freel RW, Hatch M, Green M, Soleimani M (2006) *Am J Physiol* 290:G719–G728.
10. Jiang Z, Asplin JR, Evan AP, Rajendran VM, Velazquez H, Nottoli TP, Binder HJ, Aronson PS (2006) *Nat Genet* 38:474–478.
11. Royaux IE, Wall SM, Karniski LP, Everett LA, Suzuki K, Knepper MA, Green ED (2001) *Proc Natl Acad Sci USA* 98:4221–4226.
12. Xie Q, Welch R, Mercado A, Romero MF, Mount DB (2002) *Am J Physiol* 283:F826–F838.
13. Satoh H, Susaki M, Shukunami C, Iyama K-i, Negoro T, Hiraki Y (1998) *J Biol Chem* 273:12307–12315.
14. Scott DA, Wang R, Kreman TM, Sheffield VC, Karniski LP (1999) *Nat Genet* 21:440–443.
15. Scott DA, Karniski LP (2000) *Am J Physiol* 278:C207–C211.
16. Shcheynikov N, Wang Y, Park M, Ko SBH, Dorwart M, Naruse S, Thomas PJ, Muallem S (2006) *J Gen Physiol* 127:511–524.
17. Chernova MN, Jiang L, Friedman DJ, Darman RB, Lohi H, Kere J, Vandorpe DH, Alper SL (2005) *J Biol Chem* 280:8564–8580.
18. Jiang Z, Grichtchenko II, Boron WF, Aronson PS (2002) *J Biol Chem* 277:33963–33967.
19. Zheng J, Shen W, He DZ, Long KB, Madison LD, Dallos P (2000) *Nature* 405:149–155.
20. Dallos P, Fakler B (2002) *Nat Rev Mol Cell Biol* 3:104–111.
21. Brownell WE, Bader CR, Bertrand D, de Ribaupierre Y (1985) *Science* 227:194–196.
22. Fettiplace R, Hackney CM (2006) *Nat Rev Neurosci* 7:19–29.
23. Dallos P, Evans BN, Hallworth R (1991) *Nature* 350:155–157.
24. Iwasa KH (2001) *Biophys J* 81:2495–2506.
25. Oliver D, He DZ, Klocker N, Ludwig J, Schulte U, Waldegger S, Ruppersberg JP, Dallos P, Fakler B (2001) *Science* 292:2340–2343.
26. Oliver D, Schaechinger T, Fakler B (2006) *Novartis Found Symp* 273:244–253.
27. Song L, Seeger A, Santos-Sacchi J (2005) *Biophys J* 88:2350–2362.
28. Albert JT, Winter H, Schaechinger TJ, Weber T, Wang X, He DZZ, Hendrich O, Geisler H, Zimmermann U, Oelmann K, *et al.* (2007) *J Physiol (London)*, 10.1113/jphysiol.2007.127993.
29. Weber T, Gopfert MC, Winter H, Zimmermann U, Kohler H, Meier A, Hendrich O, Rohbock K, Robert D, Knipper M (2003) *Proc Natl Acad Sci USA* 100:7690–7695.
30. Weer PD, Gadsby DC, Rakowski RF (1988) *Annu Rev Physiol* 50:225–241.
31. Accardi A, Miller C (2004) *Nature* 427:803–807.
32. Kakehata S, Santos-Sacchi J (1996) *J Neurosci* 16:4881–4889.
33. Bissig M, Hagenbuch B, Stieger B, Koller T, Meier P (1994) *J Biol Chem* 269:3017–3021.
34. Lee A, Beck L, Markovich D (2003) *DNA Cell Biol* 22:19–31.
35. Quondamatteo F, Krick W, Hagos Y, Kruger M-H, Neubauer-Saile K, Herken R, Ramadori G, Burckhardt G, Burckhardt BC (2006) *Am J Physiol* 290:G1075–G1081.
36. Darling I, Mammarella M, Chen Q, Morris M (1994) *Drug Metab Dispos* 22:318–323.
37. Grassl SM (1996) *Biochim Biophys Acta* 1282:115–123.
38. Markovich D, Bissig M, Sorribas V, Hagenbuch B, Meier P, Murer H (1994) *J Biol Chem* 269:3022–3026.
39. Karniski LP, Lotscher M, Fucentese M, Hilfiker H, Biber J, Murer H (1998) *Am J Physiol* 275:F79–F87.
40. Pusch M, Neher E (1988) *Pflügers Arch* 411:204–211.
41. Stewart CE, Hudspeth AJ (2000) *Proc Natl Acad Sci USA* 97:454–459.
42. Manley GA (2001) *J Neurophysiol* 86:541–549.
43. Muallem D, Ashmore J (2006) *Biophys J* 90:4035–4045.